ISBN: 978-3-95450-262-2 ISSN: 2673-5350 doi: 10.18429/JACoW-IBIC2025-WEPCO12

DEVELOPMENT OF A RECTANGULAR DIAGONAL CUT–PLANE BPM FOR THE CSNS-II INJECTION UPGRADE *

M. A. Rehman, X. Nie, Z. Xu, R. Liu, M. Liu, F. Li, B. Zhang, R. Yang, R. J. Yang†
Institute of High Energy Physics, Chinese Academy of Sciences (CAS), Beijing, China
also at China Neutron Spallation Source, Dongguan, China

Abstract

As a part of the CSNS-II upgrade, an improved injection scheme will be implemented to mitigate the space charge effect. To precisely measure the transverse beam position during injection, painting, and storage in the Rapid Cycling Synchrotron (RCS), a large-aperture (260 mm × 180 mm) Beam Position Monitor (BPM) is essential. The rectangular cut-plane BPM was selected for its excellent linearity over a large area and high signal-to-noise ratio (SNR). Due to limited space in the injection section, the BPM must be integrated into the AC steering magnet. To prevent thermal heating from eddy current flow, a rib structure has been incorporated into the BPM's outer body. The BPM was designed using numerical simulation codes. This paper details the simulation, design, and experimental results of the diagonal cut-plane BPM.

INTRODUCTION

The China Spallation Neutron Source (CSNS) [1, 2] is a major facility designed to generate intense pulsed neutron beams, supporting diverse scientific and industrial applications. Its accelerator system comprises three key components: an 80 MeV linear accelerator (linac), a 1.6 GeV Rapid Cycling Synchrotron (RCS), and a solid tungsten target station. The linac produces an 80 MeV H^- beam, which is injected into the RCS via a multi-turn charge exchange mechanism. The RCS accelerates the beam to 1.6 GeV, achieving a beam intensity of 1.56×10^{13} protons per pulse and a power output of 100 kW. Recent upgrades, including the integration of harmonic cavities, have increased the beam power to 170 kW [3].

As part of the CSNS-II upgrade, significant hardware improvements are planned to increase the beam power to 500 kW. A critical component of this upgrade involves boosting the beam energy in the linac from 80 MeV to 300 MeV, achieved through the implementation of superconducting cavities. To ensure precise measurement of the transverse beam position, phase, and energy in the new superconducting section of the linac, shorted stripline Beam Position Monitors (BPM) [5, 6] will be utilized. The parameters of CSNS and CSNS-II are summarized in Table 1.

A new injection painting scheme has been proposed [4] for CSNS-II to mitigate injection beam losses and space charge effects. To ensure accurate and precise transverse beam position measurements during injection, painting, and storage in the RCS, a large-aperture BPM is essential. The rectangular cut-plane BPM has been selected due to its excellent linearity over a large area, high signal-to-noise ratio (SNR), and compact mechanical structure, which also allows for integration into the corrector magnet. Since the BPM must be installed within the AC corrector magnet, eddy currents induced by the magnet can cause thermal heating. To address this, a special discontinuous structure has been incorporated into the BPM's outer body to minimize eddy current-induced heating.

Table 1: CSNS and CSNS–II RCS Parameters

Parameters	CSNS	CSNS–II	Units
Beam Power	100	500	kW
Injection Energy	80	300	MeV
Ring Circumference	227.92	227.92	m
Extraction Energy	1.6	1.6	GeV
Repetition Rate	25	25	Hz
f_{RF}	1.02-2.44	1.02-2.44	MHz
Number of Bunches	2	2	
Beam Intensity	1.56×10^{13}	7.8×10^{13}	ppb

Table 2: Diagonal Cut-plane BPM Parameters

Parameters	Values
Aperture	260 mm × 180 mm
Position Accuracy	1 % half of Aperture
Position Resolution	200 µm

DESIGN AND SIMULATIONS OF DIAGONAL CUT–PLANE BPM

The BPM in the injection region must provide transverse position measurements for the injection, painting, and circulating beam, which has a horizontal offset of approximately ±30.25 mm and a vertical offset of up to ±15 mm. Therefore, the horizontal and vertical apertures of the BPM were set to 260 mm and 180 mm, respectively, allowing for a larger acceptance during beam orbit tuning. The required position measurement accuracy is 1% of the half-aperture of the BPM. Due to stringent space requirements in the injection area, the BPM must also be installed inside the AC corrector magnet. To satisfy all the above requirements, a rectangular-shaped diagonal cut-plane BPM was chosen. The design parameters of the BPM are listed in Table 2.

* Work supported by National Science Foundation for Young Scientists of China (12305166).
† yangrenjun@ihep.ac.cn

ISBN: 978-3-95450-262-2 ISSN: 2673-5350 doi: 10.18429/JACoW-IBIC2025-WEPCO12

The diagonal cut-plane BPM is a capacitive pick-up. The passage of a charged particle beam induces an image current on the electrically isolated electrode, which is proportional to the distance between the electrode and the beam, the beam intensity, and the electrode area. The induced voltage in the frequency domain across the resistor R is given by [7]

$$V(\omega) = Z_t(\omega, \beta) I_{\text{beam}}(\omega), \tag{1}$$

where $Z_t(\omega, \beta)$ is the longitudinal transfer impedance, and $I_{\text{beam}} = I_0 e^{i\omega t}$ is the current distribution of the beam. The longitudinal transfer impedance $Z_t(\omega, \beta)$ can be expressed as

$$Z_t(\omega, \beta) = \frac{1}{\beta c}\frac{1}{C}\frac{A}{2\pi a}\frac{i\omega RC}{1 + i\omega RC}, \tag{2}$$

where $\beta = v/c$, v is the speed of the proton, c is the speed of light, C is the capacitance of the electrode, A is the area of the electrode, a is the distance from the beam center to the electrode, and ω is the angular frequency. Note that the longitudinal transfer impedance $Z_t(\omega, \beta)$ depends on frequency, the velocity of the beam particles, and geometric factors. This results in a larger signal amplitude for the BPM with a lower capacitance of the electrode, lower beam velocity, and a larger electrode area. The horizontal and vertical apertures of the electrodes are 260 mm and 180 mm, respectively. The thickness of the electrode is 1 mm, while the lengths of the horizontal and vertical electrodes are 137.7 mm and 83.4 mm, respectively. The thickness of the outer grounded body of the BPM is 15 mm, with ribs added to provide a mechanically rigid structure for the electrodes. The 3D model of the BPM electrodes is shown in Fig. 1.

The capacitance of the electrode depends on the distance between the outer surface of the electrode and the grounded body. This distance is maintained using long ceramic bars (Al_2O_3, 99 %) placed longitudinally along the BPM. The relative permittivity (ϵ_r) of the ceramic is approximately 9.9. The capacitance of the electrodes was simulated using the numerical code CST-ES [8]. Note that the capacitance increases with the addition of the ceramic bars due to the higher relative permittivity. The distance between the electrode and the grounded body was chosen to be 4 mm. The capacitances of the horizontal and vertical electrodes are 260 pF and 185 pF, respectively.

The electromagnetic coupling or cross-talk (S_{21}) between two electrodes cause the intrinsic offsets, reduce the difference signal of the two opposing electrodes and also results in lower BPM resolution. The cross talk between two electrodes was studied using the CST-MW [8]. The cross talk for the two horizontal electrodes with the gap of 6 mm for the f_{RF} (1.02–2.44 MHz) is −35 dB. Which results in finite intrinsic transverse offset. In order to reduce the cross-talk a grounded separation electrode of length 3 mm is placed between horizontal and vertical electrodes. The grounded separation electrode is 1.25 mm away from the isolated horizontal and vertical electrodes. The cross talk between the electrodes reduced to −44.07 dB with the grounded separation electrode. The simulated cross-talk (S_{21}) between the two horizontal electrodes is shown in Fig. 2.

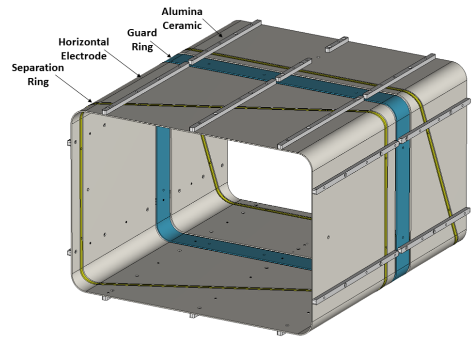

Figure 1: The 3D model of the horizontal and vertical electrodes of the diagonal cut-plane BPM is shown. The two opposing electrodes (horizontal and vertical) are separated by grounded separation electrodes to reduce inter-electrode coupling. A grounded guard has been placed between the horizontal and vertical electrodes to prevent coupling between transverse planes.

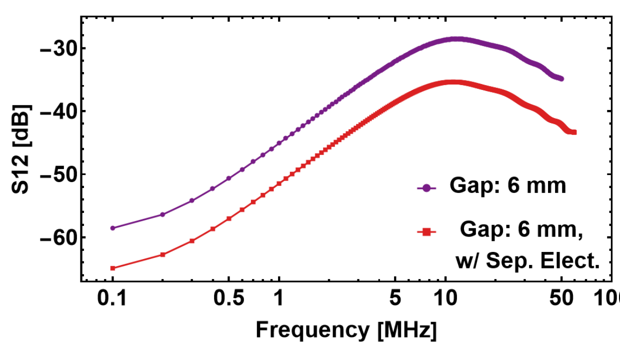

Figure 2: The electromagnetic coupling between the two horizontal electrodes is shown. The gap between the two electrodes was optimized to a value of 6 mm. The isolation between the two electrodes at the bunching frequency of 2.44 MHz is −35 dB. The addition of a grounded separation electrode increases the isolation between the electrodes to −44.07 dB at the bunching frequency of 2.44 MHz.

EDDY CURRENT

As described in the earlier section, the BPM must be installed inside the AC corrector magnet due to the limited available space in the injection region of CSNS-II. However, the AC magnet's time-varying magnetic field, with a strength of 100 G and a repetition frequency of 25 Hz, induces eddy currents on the BPM, resulting in power loss. The power loss caused by the eddy currents was simulated using CST. For an outer body made of SUS304 with a thickness of 10 mm and a conductivity of 1.389×10^6 S/m, the power loss is 40.4 W. To reduce the power loss in the outer body, a thinner outer body with a thickness of 3 mm and ribs with a thickness of 10 mm was considered, which reduced the power loss to 18 W.

ISBN: 978-3-95450-262-2 ISSN: 2673-5350 doi: 10.18429/JACoW-IBIC2025-WEPCO12

To further reduce the power loss a Ti–alloy (Ti-6Al-4V) with the lower conductivity 5.8×10^5 S/m was simulated. The lower conductivity of Ti-alloy results into lower power loss of about 2.5 W in the body of the BPM.

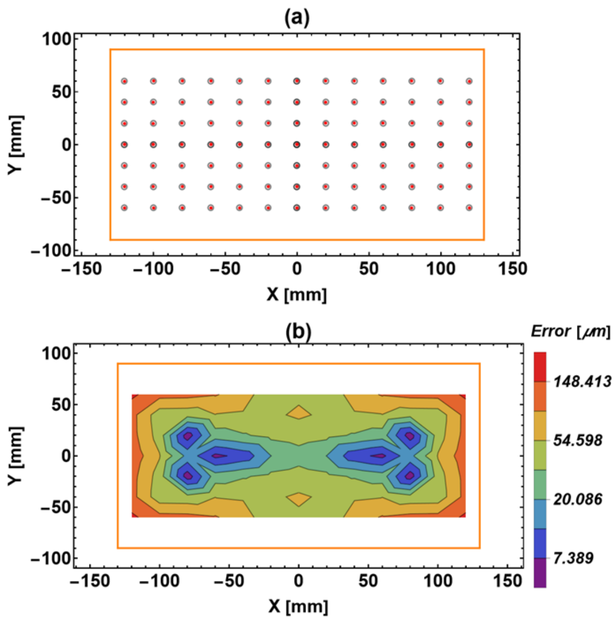

Figure 3: (a) Linear fitting to the simulated transverse raw data of the BPM. (b) Two-dimensional error map of the simulated positions with the linear fitting, showing a maximum position error of only 148 µm.

POSITION CHARACTERISTICS

In order to calculate the position response and linearity of the BPM, a proton beam with realistic parameters was simulated using the CST-Wakefield solver. The computed signals from each electrode at different transverse positions were obtained. The obtained time-domain signals were integrated for further analysis. The difference-over-sum formula was used to calculate the transverse position of the beam according to the following equations [7, 9]:

$$x = a_0 + a_1 \frac{U_{\text{right}} - U_{\text{left}}}{U_{\text{right}} + U_{\text{left}}}, \tag{3}$$

$$y = b_0 + b_1 \frac{U_{\text{top}} - U_{\text{bottom}}}{U_{\text{top}} + U_{\text{bottom}}}, \tag{4}$$

where U_{right}, U_{left}, U_{top}, and U_{bottom} are the measured signals from the right, left, top, and bottom electrodes of the BPM, respectively. The coefficients a_0, b_0, a_1, and b_1 are obtained through linear fitting. Here, a_0 and b_0 represent the horizontal and vertical offsets of the BPM, while a_1 and b_1 are the first-order coefficients used to determine the transverse position. The mapping results and absolute errors are shown in Fig. 3 (a) and (b), respectively. The maximum position error is only 148 µm, which is better than the required accuracy of 1 % of half the aperture.

ELECTRODE CROSS-TALK MEASUREMENT

The BPM was manufactured, and the cross-talk between the electrodes was measured using a vector network analyzer (VNA, Keysight E5061B) [10]. The measured cross-talk between the two horizontal electrodes was below −42.5 dB in the frequency range of 1.02–2.44 MHz, which is approximately 1.7 % higher than the simulated value of −44.07 dB. The measured S_{21} parameters are shown in Fig. 4.

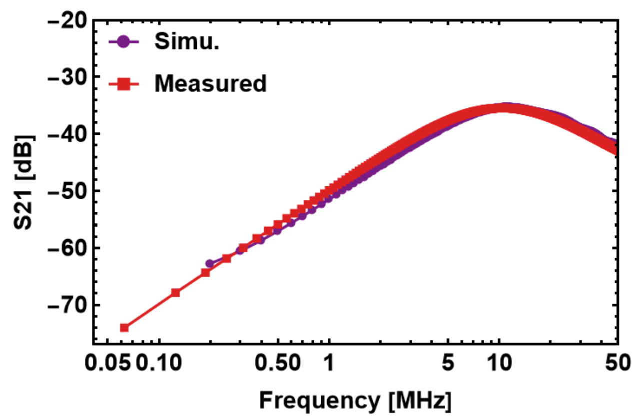

Figure 4: The simulated and measured cross-talk (S_{21}) of two opposing horizontal electrodes. The measured isolation between the electrodes is −42.5 dB.

SUMMARY

As part of the CSNS-II power upgrade, an improved injection scheme has been implemented. A rectangular, diagonally cut-plane BPM was designed and simulated to measure the transverse positions of the injected, painting, and stored beams in the RCS. The electrode capacitance was optimized by adjusting the gap between the electrodes and the grounded enclosure. High-purity ceramic (99 % Al_2O_3) was incorporated between the isolated electrodes and the grounded enclosure to secure the electrodes. Numerical simulations were used optimized the inter-electrode isolation to −44.07 dB through the addition of a grounded separation electrode. A discontinuous rib structure was introduced on the outer grounded enclosure to mitigate eddy-current-induced power losses from the AC corrector magnet. The simulations were performed to evaluate the BPM's position sensitivity, linear fitting of the data yielded a maximum error of 148 µm, meeting the required position accuracy. The BPM was fabricated, and its S-parameters were measured using a VNA. The measured electrode cross-talk was −42.53 dB.

ACKNOWLEDGMENTS

We thank Prof. S. Wang and Prof. L. Ma from IHEP as well as P. Forck from GSI, for fruitful discussions.

REFERENCES

[1] J. Wei *et al.*, "China Spallation Neutron Source: Design, R&D and Outlook", *Nucl. Instrum. Methods Phys. Res. A*,

ISBN: 978-3-95450-262-2 ISSN: 2673-5350 doi: 10.18429/JACoW-IBIC2025-WEPCO12

vol. 600, no. 1, pp. 10–13 2009. doi:10.1016/j.nima.2008.11.017

[2] W. Sheng *et al.*, "Introduction to the overall physics design of CSNS accelerators", *Chin. Phys. C*, vol. 33, no. S2, p. 1, 2009. doi:10.1088/1674-1137/33/S2/001

[3] L. Huang *et al.*, "Intense Beam Issues in CSNS Accelerator Beam Commissioning", in *Proc. HB'23*, Geneva, Switzerland, Oct. 2023, pp. 16–22. doi:10.18429/JACoW-HB2023-MOA1I3

[4] M.Y. Huang *et al.*, "Performance of the correlated painting based on the mechanical structure of the anticorrelated painting scheme", *Phys. Rev. Accel. Beams*, vol. 25, p. 110401, 2022. doi:10.1103/PhysRevAccelBeams.25.110401

[5] M. A. Rehman *et al.*, "Development and operation of shorted stripline BPM system for the CSNS LINAC", *Nucl. Instrum. Methods Phys. Res. A*, vol. 1080, p. 170671, 2025. doi:10.1016/j.nima.2025.170671

[6] M. A. Rehman *et al.*, "Development of stripline-type beam position monitor system for CSNS-II", *Proc. IBIC'24*, Beijing, China, Sep. 2024, pp. 98–101. doi:10.18429/JACoW-IBIC2024-TUP25

[7] P. Forck, P Kowina, and D Liakin, "Beam Position Monitors", in *CERN Accelerator School: Beam Diagnostics*, CERN, Geneva, Switzerland, 2009, p. 187. doi:10.5170/CERN-2009-005.187

[8] CST, https://www.3ds.com/products/simulia/cst-studio-suite

[9] Robert E. Shafer. "Beam position monitor sensitivity for low β-beams", in *AIP Conf. Proc.*, vol. 319, Sante Fe, New Mexico, USA, Oct. 1993, pp. 303–308. doi:10.1063/1.46975

[10] Keysight, https://www.keysight.com